Uplink coexistence for high throughput UAVs in cellular networks

Zaki-Hindi, Ayat; Amorim, Rafhael; Kovács, István; Wigard, Jeroen

Published in:
IEEE Global Communications Conference (Globecom) 2022

Publication date:
2022

Uplink coexistence for high throughput UAVs in cellular networks

Ayat Zaki-Hindi[1], Rafhael Amorim[2], István Z. Kovács[2], Jeroen Wigard[2]
[1] Aalborg University, Aalborg, Denmark
[2] Nokia, Aalborg, Denmark
azh@es.aau.dk, {rafhael.medeiros_de_amorim, istvan.kovacs, jeroen.wigard}@nokia.com

***Abstract*—We focus in this paper on Cellular-connected Uncrewed Aerial Vehicles (UAVs) in a scenario of a camera-equipped UAV, streaming a live event. The UAV coexists with a large number of ground User Equipment (gUEs) belonging to people attending the same event, and using the network to transmit their data. Hence the cellular network must satisfy the high data rate demand of both the UAV and gUEs. For that, we explore interference mitigation solutions, and propose a novel algorithm for UAV cell-selection which minimizes the impact of the UAV to the concerned serving cell. The results demonstrate an uplink data-rate gain of 32% for gUEs in the crowded cell, compared to the standard algorithm, while achieving a target UAV throughput of 20 Mbps. This comes at a cost of increased UAV transmission power of 50% and a slight data rate degradation for gUEs in neighboring cells, up to 13%.**

I. Introduction

Thanks to the easy deployment and high 3D mobility of Uncrewed Aerial Vehicles (UAVs), many useful services have emerged, such as last-mile package delivery, surveillance, and streaming of live events [1]. To ensure a high reliability and high data rates for such applications, cellular-connected UAVs have been studied [2], where the UAV is considered as an aerial User Equipment (UE) in a cellular network, e.g., 5G networks.

UAVs can be used to stream from live events like concerts, where a camera-equipped UAV seeks a high uplink data rate to ensure a good quality of the streamed video. At the same time, there might be many ground UEs (abbreviated gUEs) at the event, leading to their serving cell being highly loaded. In this case, the UAV which is located in proximity may compromise the performance of gUEs in this hotspot cell.

On one hand, if the UAV is sharing the same resources as the serving cell of gUEs, then the UAV occupies the majority of the resources to satisfy its performance requirements, leaving the large number of gUEs with a poor Quality of Service (QoS). On the other hand, if the UAV connects to a different cell while in proximity to the hotspot, then the generated interference from the UAV degrades the reliability of decoding of the gUEs signals that are transmitted over the same resources, leading to a poor QoS as well.

We can partially remedy this interference problem by using beamforming on the UAV side [3], or by using downtilted directional antenna [4]. A directional antenna focuses the radiated energy spatially in one mainbeam, limiting the radiation in other directions. In our case, the direction of the UAV's mainbeam is critical in the cell selection process, i.e., if it is directed towards the hotspot cell's Base Station (BS), then the created interference level would be equivalent to the omni-directional case and the gUEs' uplink performance will still suffer from a high interference level compromising their performance.

The interference mitigation of cellular-connected UAVs has been addressed in the literature. For instance, the use of a directional antenna on the UAV side is proven experimentally to enhance the interference mitigation towards neighboring cells, in [5]. Furthermore, the authors in [6] propose an inter-cell interference coordination (ICIC) scheme to maximize the weighted sum-rate of the UAV and gUEs via jointly optimizing the UAV's uplink cell associations and transmit power allocations over multiple resource blocks.

In this paper, we address the co-existence issue of one UAV with a hotspot in the same coverage area. In particular, when the rate-demanding UAV is located near a high traffic cell, that needs to provide an acceptable performance to its users. Meanwhile, other cells are considered partially loaded and can be used to offload the UAV's traffic. Our goal is to minimize the impact of the UAV to the hotspot cell, by proposing a novel algorithm for the UAV cell selection, based on the UAV's location and interference signal level to the hotspot, while equipped with a directional antenna.

The remainder of this paper is organized as follows. In Section II, we describe the scenario and system model, then we introduce in Section III, the traditional and proposed UAV's cell selection algorithms. In Section IV, we descrive the system-level simulator and present the main resluts. We finally conclude the paper in Section V.

II. Scenario and system model

We consider a simulated rural environment with three-sector BSs, where sectors are equivalent to cells. The layout is shown in figure 1 with parameters in Table I, similar to the considered scenarios in [7]. The network is composed of seven main cells, surrounded by two outer-rings of cells, with a total of 37 cells, to create realistic

978-1-6654-3540-6/22/$31.00

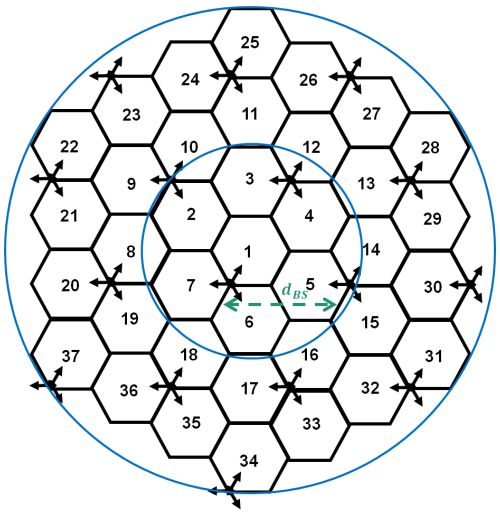

Figure 1: Network layout

interference conditions for the 7 middle cells. Each cells BS is denoted by $BS_i, i \in \{1, 2, \ldots, 37\}$, represented by an arrow in the figure. The distance between two BSs is constant and denoted by d_{BS}.

An outdoor event takes place in one of the 7 inner cells, e.g., cell 1, which is expected to serve a large number of gUEs and to provide them with an acceptable performance. We denote this cell by the hotspot, noting that we use the term hotspot here differently from the conventional one as a private micro-cell.

In proximity to the hotspot cell and within the inner cell ring, a UAV is flying and filming the event with an onboard camera. The generated video data must be conveyed to the terrestrial network with a target data rate: R_{target}, to ensure a good streaming quality. The main output Key Performance Indicator (KPI) looked at is the data rate (throughput) of the UAV and gUEs.

We assume that all cells are operating on the same frequency bandwidth W and all transmitters (gUEs and UAV) perform Open Loop Power Control (OLPC) [8] to adapt their transmission power. For simplicity, we consider full-bandwidth transmission per Transmission Time Interval (TTI). Since every BS schedules one UE at most per TTI, we model the gUE performance by assuming one gUE per cell, denoted by $u_i, i \in \{1, \ldots, 37\}$. To get the real data rate per gUE, the realised data rate needs to be divided by the number of gUEs.

The data rate is evaluated for one realization of the network, i.e., fixed locations of the UAV and gUEs, of a duration of T seconds. We denote the horizontal-plane coordinates of the UAV, BS_i and u_i by (x_{UAV}, y_{UAV}), (x_i, y_i) and (x_{u_i}, y_{u_i}), respectively. The heights of the UAV, BS_i and u_i are respectively denoted by h_{UAV}, h_{BS_i} and h_{u_i}, and are fixed for all realizations. The horizontal distance between BS_i and u_i (or the UAV) is calculated as: $d_i(u_i) = \sqrt{(x_i - x_{u_i})^2 + (y_i - y_{u_i})^2}$.

Table I: Numerical values of the system parameters

Environment parameters			
d_{BS}	2 km	h_{UAV}	100 m
h_{BS_i}	35 m	h_{u_i}	1.5 m
W	10 MHz	f_W	900 MHz
M	50	P_{max} (over W)	23 dBm
R_{target}	20 Mbps	P_N (over W)	-104 dBm
W_{eff}	0.75	SNR_{eff}	1.25
N_{MC}	100 000	N_T	100
$N_{SF}(UAV)$	5000	$N_{SF}(gUE)$	10 000
BS and UAV antenna patterns			
$A_m^{horizontal}$	20 dB	$\Theta_{3dB}^{horizontal}$	65^o
$A_m^{vertical}$	15 dB	$\Theta_{3dB}^{vertical}$	7.5^o
A_m^{UAV}	20 dB	Θ_{3dB}^{UAV}	65^o
G_{BS}	18 dB	G_{UAV}	6 dB
Shadow fading parameters			
ρ_{gUE}	0.3	ρ_{UAV}	0.3
σ_{gUE}	6 dB	σ_{UAV}	4 dB
D_{gUE}	50 m	D_{UAV}	500 m
Transmit power OLPC			
γ_{gUE}	3.5	γ_{UAV}	2
α_{gUE}	0.7	α_{UAV}	1
$P_{0,gUE}$ PRB	-72 dBm	$P_{0,UAV}$ PRB	-100 dBm

The UAV is assumed connected to cell $\ell, \ell \in \{1, 2, \ldots, 37\}$ according to a cell selection algorithm (detailed in the following section), and BS_ℓ provides the UAV with the needed resources to achieve R_{target}.

In one realization of the network, each u_i is active with probability $P_{active}(i)$, to simulate the different loads of the cells, where we consider:

$$P_{active}(i) = \begin{cases} 1 \text{ if } i \text{ is the hotspot} \\ 0.3 \text{ otherwise} \end{cases} \quad (1)$$

Regardless of u_ℓ's activity, BS_ℓ prioritizes the UAV's traffic and allocates τ seconds (of T) to the UAV, where τ is calculated based on R_{target} and the channel capacity.

In the sequel, we explain in details the system components and performance evaluation steps. We use the notation $f_j(u_i)$ to indicate that the function f is being evaluated for cell j when u_i is connected to cell i, and the UAV is connected to cell ℓ.

A. Antenna pattern

Each sector (cell) is equipped with a directional antenna of 120^o horizontal width.We consider a simplified antenna pattern following the recommendations in [9] which consists of one main-lobe and no side lobes. The relative antenna gain $A(\Theta)$ (dB) in the direction $\Theta, -180^o \leq \Theta \leq 180^o$, is given by equation (2), where G is the beamforming gain, A_m is the maximum attenuation and Θ_{3dB} is the 3-dB beamwidth.

$$A(\Theta) = G - \min\left[12\left(\frac{\Theta}{\Theta_{3dB}}\right)^2, A_m\right]. \quad (2)$$

We denote the horizontal and vertical antenna attenuation by $A^{horizontal}(\Theta)$ and $A^{vertical}(\Theta)$, respectively, and both are illustrated in Figure 2, along with a practical

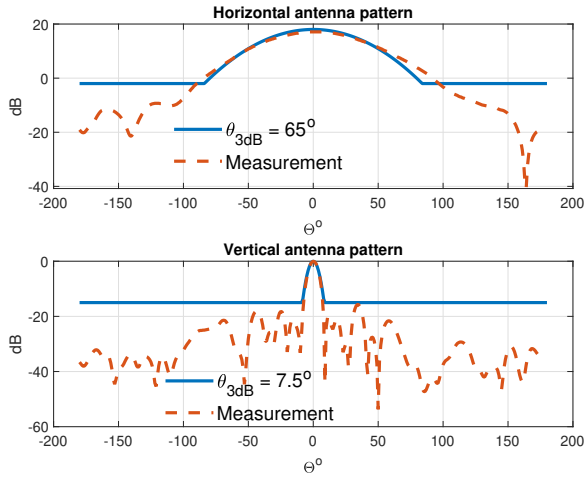

Figure 2: Horizontal and vertical BS antenna pattern

antenna pattern, where $G^{horizontal} = 18$, $G^{vertical} = 0$, $A_m^{horizontal} = 20$ dB, $A_m^{vertical} = 15$ dB, $\Theta_{3dB}^{horizontal} = 65^o$ and $\Theta_{3dB}^{vertical} = 7.5^o$ [7]. The total antenna attenuation is: $A_{BS} = A^{horizontal}(\Theta) + A^{vertical}(\Theta)$.

Sector antennas are usually slightly downtilted [7] with $\Theta_{downtilt}$, to optimize the performance for gUEs, which affects the performance of aerial UEs, since they will be served through the side lobes in some locations. For the considered UAV's directional antenna, we use the same pattern in equation (2), for the horizontal plane only. We ignore the vertical attenuation because the antenna is downtilted towards the BSs. We denote the UAV's antenna attenuation by A_{UAV} with beamforming gain of G_{UAV}.

B. Shadow fading and pathloss

The shadow fading, also known as large scale fading, is an incorporation of the environment effect on the radio propagation, such as buildings, hills, and other obstacles. It depends on many factors, including the type of environment (urban, rural, ...), the used radio frequency and the probability of LoS between the sender and receiver.

For our study, we consider the bi-dimensional correlated model proposed in [10]. In this model, maps (matrices) of the layout size are generated randomly from a normal distribution, then filtered with 2D Finite Impulse Response (FIR) to introduce a cross-correlation between the different BSs. The most important parameters of this model are the coorelation factor ρ, the Normal distribution $\mathcal{N}(0, \sigma^2)$ and the decorrelation distance D, which are different between the UAV and the gUEs, because of the different probabilities of LoS.

For that, we generate two different maps for each BS, one for the UAV and one for the gUES. The maps between BS_i and gUE $u_i, i \in \{1, \ldots, 37\}$ (or the UAV) are denoted by $SF_i(u_i)$ (or $SF_i(UAV)$).

The pathloss (in dB) between u_i (or the UAV) and BS_i is modeled by equation (3), where $ct = \frac{4\pi f_W}{c}$ is a constant that depends on the operating frequency f_W and the light speed c, $SF_i(u_i)$ is the slow shadow fading between u_i and BS_i, and γ_{u_i} is the pathloss exponent which depends on the UE height [11].

$$PL_i(u_i) = 20\log_{10}(ct) + 10\gamma_{u_i}\log_{10}(d_i(u_i)) - SF_i(u_i) \quad (3)$$

C. Transmit power

UEs determine their transmit power using OLPC based on the pathloss and antenna attenuation measurements, with some pre-defined parameters. The advantage of OLPC is that the UEs can set their uplink transmission power without the need of feedback from the BS.

u_i can calculate its transmit power (in dBm) with OLPC following the formula in (4) [8], where M is the total number of frequency Resource Blocks (RBs), noting that the power is limited to P_{max}: the maximum allowed transmission power. The parameter $\alpha_{gUE} \in [0, 1]$ is the pathloss compensation factor.

$$\begin{aligned} P_{Tx}(u_i) = \min\{P_{max}, P_{0,gUE} + 10\log_{10}(M) \\ + \alpha_{gUE}\left[PL_i(u_i) - A_{BS_i}(\Theta(u_i))\right]\} \end{aligned} \quad (4)$$

Equation (4) indicates that the further u_i is from BS_i, the higher it transmits power. We note that the UAV compensates for its antenna gain when it is equipped with a directional one, by adding the term $-\alpha_{UAV}G_{UAV}$ to equation (4), after replacing u_i by UAV; the attenuation is of 0 dB because it is directed towards the BS.

D. Received signal

Every cell receives many superposed signals from different users transmitting simultaneously over the same resources. Ideally, the intended signal from u_i to BS_i has the highest power level and the cell is able to decode it reliably.

We can calculate the useful received signal (in dBm) from u_i to BS_i from equations (5).

$$S_i(u_i) = P_{Tx}(u_i) + A_{BS_i}(\Theta(u_i)) - PL_i(u_i) \quad (5)$$

On the other hand, the interfering signal towards BS_i generated from $u_j, j \neq i$ that is connected to BS_j can be calculated as.

$$S_i(u_j) = P_{Tx}(u_j) + A_{BS_i}(\Theta(u_j)) - PL_i(u_j) \quad (6)$$

For the directional-antenna UAV case, the useful signal towards BS_ℓ and the interfering one towards BS_i are given by equations (7- 8).

$$\begin{aligned} S_\ell(UAV) = P_{Tx}(UAV) + A_{BS_\ell}(\Theta(UAV)) \\ + G_{UAV} - PL_\ell(UAV) \end{aligned} \quad (7)$$

$$\begin{aligned} S_i(UAV) = P_{Tx}(UAV) + A_{BS_i}(\Theta_i(UAV)) \\ + A_{UAV}(\Theta(BS_i)) - PL_i(UAV) \end{aligned} \quad (8)$$

E. Data rate

The data rate is the amount of data transmitted between a sender and a receiver over a limited bandwidth in a time interval, with a certain block error rate (BLER). It is mainly influenced by the available frequency and time resources, denoted by W (in Hertz) and T (in seconds), respectively, and the signal to interference and noise ratio (SINR) over the time-frequency resources. In wireless networks, additive white Gaussian noise (AWGN) channel is usually considered with a noise level over the whole bandwidth, denoted by P_N.

We introduce the boolean $active(j)$ to indicate whether u_j is active or not in one T. During T, active $u_i, i \neq \ell$ transmits over the whole time-frequency resources, and u_ℓ shares the time resources with the UAV, where the UAV occupies the channel during τ seconds, and u_ℓ (if active) during $T - \tau$ seconds. In this case, cell $i, i \neq \ell$ receives a sum of interfering signals from active gUEs during $T - \tau$, given by $I_i(gUE) = \sum_{j \neq i} active(j) S_i(u_j)$, and from active gUES excluding u_ℓ and the UAV during τ, given by $I_i(UAV) = I_i(gUE) - active(\ell) S_i(u_\ell) + S_i(UAV)$.

The data rates of u_ℓ, $u_i, i \neq \ell$ and the UAV can be calculated from equations (9-11), respectively, using Shannon's channel capacity formula. Note here that all quantities are expressed in linear domain instead of dB. We normalise the time duration to one second, τ/T and $1 - \tau/T$, in order to get the data rate in bits per second (bps) unit.

$$R(u_\ell) = \frac{T - \tau}{T} \times W \times \log_2 \left(1 + \frac{S_\ell(u_\ell)}{I_\ell(gUE) + P_N}\right) \quad (9)$$

$$R(u_i) = \frac{T - \tau}{T} \times W \times \log_2 \left(1 + \frac{S_i(u_i)}{I_i(gUE) + P_N}\right) + \frac{\tau}{T} \times W \times \log_2 \left(1 + \frac{S_i(u_i)}{I_i(UAV) + P_N}\right) \quad (10)$$

$$R(UAV) = \frac{\tau}{T} \times W \times \log_2 \left(1 + \frac{S_\ell(UAV)}{I_\ell(gUE) + P_N}\right) \quad (11)$$

In order for the UAV to achieve its target data rate R_{target}, we adjust τ (every T) following equation (12).

$$\tau = \frac{T \times R_{target}}{W \times \log_2 \left(1 + \frac{S_\ell(UAV)}{I_\ell(gUE) + P_N}\right)} \quad (12)$$

We use a modified Shannon capacity formula for equations (9-11) that is adapted for LTE networks in [12], where W is multiplied by W_{eff} and the SINR is divided by SNR_{eff}. W_{eff} and SNR_{eff} are the bandwidth and SNR efficiency adjustments for LTE.

III. Algorithms for cell selection

We describe now the two considered algorithms for the UAV cell selection. The first being the conventional algorithm based on Reference Signal Receive Power (RSRP) data, and the second is our proposed one for a directional-antenna UAV, aiming to minimize its effect on the hotspot cell.

A. Best RSRP criteria

In this algorithm, the UAV receives the RSRP measurements from the surrounding cells, then selects the one with the maximum RSRP value. The advantages of this algorithm is minimizing the energy consumption of the UAV since its transmit power would be the lowest possible. However, this algorithm has no consideration to the hotspot needs, and may cause major performance degradation, even if the UAV is equipped with a directional antenna.

B. Minimum interference to hotspot criteria

We can protect the hotspot cell from the UAV's interference by connecting the UAV to the cell which causes the lowest interference level towards the hotspot: $\ell = \arg\min_{i \neq HS}\{S_{HS}(UAV_i)\}$, where HS denotes the hotspot, while the UAV is eqipped with a directional antenna. We exclude the hotspot from the cell selection process to avoid the rate degradation resulting from sharing the same resources. However, we add a condition that the UAV connects to the hotspot if, an only if, connecting the UAV to the hotspot causes less harm to the hotspot's rate: $R_{HS}(UAV(HS)) > R_{HS}(UAV(\ell))$. This condition is demonstrated in cases where the UAV is transmitting with a relatively high power and is located in proximity to the hotspot's BS. In this case, the UAV's antenna attenuation may not be enough to reduce the interference towards the hotspot, and the activity time of the UAV would be lower since its spectral efficiency (channel capacity) is high.

IV. Numerical evaluation

For the numerical evaluation, we perform a Monte-Carlo simulation to evaluate the average performance based on the different UAV and gUEs locations. We aim to show that our proposed algorithm for the UAV's cell selection improves the data rate of the hotspot, compared to the conventional algorithm. The numerical values are shown in Table I and the simulation process is described in algorithm 1. We denote by N_{MC} and N_T the number of Monte-Carlo iterations and the number of T intervals, respectively. The slow shadow fading maps are changed every $N_{SF}(UAV)$ iterations for the UAV and $N_{SF}(gUE)$ for the gUEs. We consider cell 1 as the hotspot, and the UAV can be located anywhere within cells 1-7. The UAV's BLER is considered of 10%, i.e., The UAV is guaranteed its target throughput of 20 Mbps in 90% of the times.

We illustrate in Figure 3 the percentage of UAV connection to each cell, following the two considered cell selection algorithms. Looking at Best RSRP, we notice that the highest percentages belong to cells 1, 2 and 5, contrary to what one might expect from Figure 1, to have an equal distribution over the first 7 cells. This is due to

Algorithm 1: System evaluation

Set system parameters;
for $m = 1$ *to* N_{MC} **do**
  if $m \mod N_{SF}(.) = 1$ **then**
    Generate new shadow fading maps (UAV/gUE);
  end
  Generate random locations for the UAV/gUEs;
  Calculate their **transmit power** from eq. (4);
  Calculate the **useful and interfering signals** from eq. (5-8), where $\ell \in \{1, \dots 37\}$;
  Select cell ℓ for the UAV according to Sect. III;
  for $k = 1$ *to* N_T **do**
    Select active gUEs $active_k$ based on eq. (1);
    Calculate τ from eq. (12);
    Calculate the **data rates** from eq. (9-11);
  end
  Calculate the **average data rates** over k;
end

the BS antenna's vertical attenuation and downtilt, and the high probability of LoS to the UAV, which spreads the coverage of the UAV away from the BS. This also explains the connection to the outer ring cells, whose BS antenna points inwards. We note that the random shadow fading also plays a role in having small differences in these percentages.

Observing Min. interference algorithm, the UAV never connects to cell 1 (the hotspot), because it requires a large amount of resources ($\tau > T/2$) and it is never beneficial for the hotspot. The UAV never connects to cells 6 and 7 neither, since they are co-site to cell 1, and the UAV's mainbeam is pointing directly towards it, causing a high interference level. Hence, when the UAV is located in the coverage area of cells 1, 6 and 7, the UAV connects to the neighboring cells, increasing their UAV connection rate compared to Best RSRP.For the rest of the UAV locations, Min interference does not deviate from Best RSRP, hence we limit our following results to the cases where the two algorithms are different.

We trace in Figure 4, the Cumulative Distribution Function (CDF) of the uplink data rate to gUE in cell 1 (the hotspot). We compare the two considered algorithms, along with the worst-case and best-case scenarios: where the UAV is equipped with an omni-directional antenna and where there is no UAV in the network, respectively. The results demonstrate the advantage of Min-interference over Best RSRP for the hotspot, bringing the CDF closer to the upper-bound with no UAV in the network.

To quantify the impact of the new algorithm on the performance of gUEs, we organize in Table II the 10th, the 50th and the 90th percentile of the served cell throughput CDF for a number of selected cells, considering the symmetry of the network layout. We note that the cell throughput for cell 1 is generally higher than the other cells due to a different assumed activity factor (100% vs 30%).

The results show that the use of UAV directional antenna is always advantageous over omni-directional one,

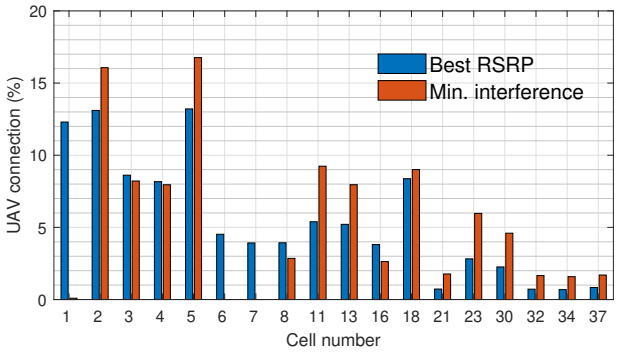

Figure 3: The percentage of UAV connection to each cell

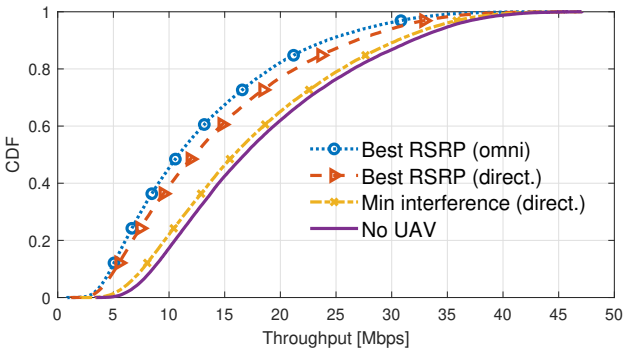

Figure 4: CDF of served data rate to gUE in cell 1

which agrees with the results presented in [5]. We focus on the difference between Min. interference and Best RSRP (direct.) performance, denoted by Gain Min.interference in Table II. The cells are divided into three main categories:

- Cells that benefit from Min. interference, which are mainly the hotspot and its co-site cells, since they do not share their resources with the UAV anymore.
- Cells that are not impacted by the used algorithm, where the UAV does not considerably change its connection to them with the used algorithm.
- Cells that suffer from a performance degradation, because of the increased UAV connection to them, and sharing their resources, represented by cell 11 in Table II.

We also note that the difference between Min. interference and the baseline with no UAV, to the hotspot, is as close as 6% at the 50th percentile, which proves the efficiency of Min. interference to the hotspot.

Regarding the price payed by the UAV in the form of transmit power, we show in Figure 5 the CDF of the UAV's transmit power (in dBm) for the different algorithms. The figure illustrates that Best RSRP (direct) is the optimal algorithm from the viewpoint of power consumption, and the penalty of Min. interference when deviating from Best RSRP (direct) is estimated by 50%, 42%, and 40% for the 10th, the 50th and the 90th percentile of the CDF, respectively (calculated in linear domain). However, the

Table II: Served cell throughput per cell for gUEs and gain of Min. interference with respect to Best RSRP (direct.)

	Algorithm	@ 10% [Mbps]	@ 50% [Mbps]	@ 90% [Mbps]
cell 1 100% load	No UAV (baseline)	8.54	16.77	31.83
	Best RSRP (omni)	4.78	10.87	24.17
	Best RSRP (direct)	5.18	12.27	26.81
	Min. interference	7.61	15.86	30.49
	Gain Min. interference	+32%	+23%	+12%
cell 2 30% load	No UAV (baseline)	1.30	3.42	9.14
	Best RSRP (omni)	0.58	1.81	5.76
	Best RSRP (direct)	0.90	2.88	8.35
	Min. interference	0.91	2.70	7.95
	Gain Min. interference	+1%	−6%	−5%
cell 3 30% load	No UAV (baseline)	1.74	4.04	9.62
	Best RSRP (omni)	1.04	2.76	7.56
	Best RSRP (direct)	1.46	3.65	9.08
	Min. interference	1.43	3.59	9.00
	Gain Min. interference	−2%	−2%	−1%
cell 6 30% load	No UAV (baseline)	1.91	4.52	9.32
	Best RSRP (omni)	1.38	3.67	8.15
	Best RSRP (direct)	1.51	3.96	8.53
	Min. interference	1.81	4.42	9.15
	Gain Min. interference	+16%	+10%	+7%
cell 11 30% load	No UAV (baseline)	1.44	4.46	8.95
	Best RSRP (omni)	0.74	2.72	6.13
	Best RSRP (direct)	1.08	4.04	8.32
	Min. interference	0.95	3.66	7.90
	Gain Min. interference	−13%	−10%	−5%

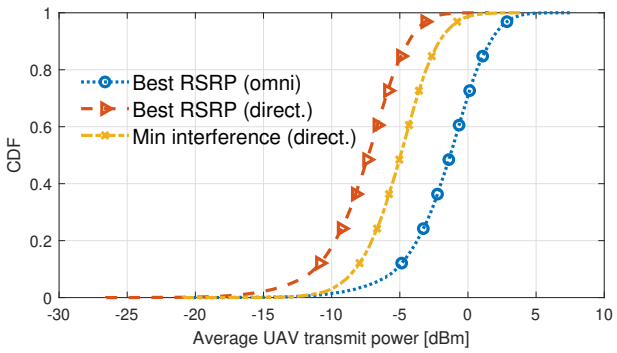

Figure 5: CDF of the UAV's transmit power

price payed for Min. interference to protect the hotspot is still considerably lower than the case where the UAV is equipped with an omni-directional antenna. At the 50th percentile, Min. interference and Best RSRP (direct) have a respective gain in power consumption of 131% and 173% over Best RSRP (omni).

V. Conclusion

We studied in this paper the co-existence of one UAV with a hotspot of gUEs in a simulated 3GPP rural scenario. The hotspot cell is characterized with a large amount of traffic coming from a large number of gUEs that demand high data rates. With the presence of the UAV's uplink interference, the performance of these gUEs can be compromised. Hence we proposed a new algorithm for UAV cell-selection, to minimize its impact on the gUEs in the hotspot. The algorithm uses a directional antenna on the UAV side,and selects the cell which minimizes the interference of the UAV to the hotspot. The algorithm is tested in a system-level simulator and is shown to have a considerable gain in the hotspot's gUE data rate, up to 32%, compared to the traditional algorithm for cell selection: Best RSRP. We further show that the data rate degradation for gUEs in some neighboring cells using this algorithm does not exceed 13%, and that the transmit power increase for the UAV is less than 50%.

References

[1] Yongs Zeng et al. Accessing from the sky: A tutorial on UAV communications for 5G and beyond. *Proceedings of the IEEE*, 107(12):2327–2375, 2019.

[2] Debashisha Mishra and Enrico Natalizio. A survey on cellular-connected UAVs: Design challenges, enabling 5G/B5G innovations, and experimental advancements. *Computer Networks*, 182:107451, 2020.

[3] Yong Zeng et al. Cellular-connected UAV: Potential, challenges, and promising technologies. *IEEE Wireless Communications*, 26(1):120–127, 2018.

[4] Tomasz Izydorczyk et al. Experimental evaluation of beamforming on uavs in cellular systems. In *2020 IEEE 92nd Vehicular Technology Conference (VTC2020-Fall)*, pages 1–5. IEEE, 2020.

[5] Rafhael Amorim et al. Measured uplink interference caused by aerial vehicles in LTE cellular networks. *IEEE Wireless Communications Letters*, 7(6):958–961, 2018.

[6] Weidong Mei et al. Cellular-connected UAV: Uplink association, power control and interference coordination. *IEEE Transactions on wireless communications*, 18(11):5380–5393, 2019.

[7] 3GPP. Study on channel model for frequencies from 0.5 to 100 ghz. *3rd Generation Partnership Project (3GPP), Tech. Rep.*, 38, 2018.

[8] Robert Mullner et al. Contrasting open-loop and closed-loop power control performance in UTRAN LTE uplink by UE trace analysis. In *2009 IEEE International Conference on Communications*, pages 1–6. IEEE, 2009.

[9] M Series. Guidelines for evaluation of radio interface technologies for IMT-Advanced. *Report ITU*, 638:1–72, 2009.

[10] Rubén Fraile et al. Mobile radio bi-dimensional large-scale fading modelling with site-to-site cross-correlation. *European transactions on telecommunications*, 19(1):101–106, 2008.

[11] Rafhael Amorim et al. Radio channel modeling for UAV communication over cellular networks. *IEEE Wireless Communications Letters*, 6(4):514–517, 2017.

[12] Preben Mogensen et al. LTE capacity compared to the shannon bound. In *2007 IEEE 65th vehicular technology conference-VTC2007-Spring*, pages 1234–1238. IEEE, 2007.